Materials Chemistry and Physics 305 (2023) 127968

Contents lists available at ScienceDirect

Materials Chemistry and Physics

journal homepage: www.elsevier.com/locate/matchemphys

TiO_2–SiO_2–Ag electrospun fibers for oxytetracycline detection by SERS

Daniela Solorio-Grajeda [a], Álvaro de Jesús Ruíz-Baltazar [b], Manuela Alejandra Zalapa-Garibay [c], Erasto Armando Zaragoza-Contreras [d], Simón Yobanny Reyes-López [a,*]

[a] Laboratorio de Materiales Híbridos Nanoestructurados, Instituto de Ciencias Biomédicas, Departamento de Ciencias Químico Biológicas, Universidad Autónoma de Ciudad Juárez, Anillo Envolvente del Pronaf y Estocolmo s/n, Zona Pronaf, Ciudad Juárez, Chihuahua, C.P. 32310, Mexico
[b] CONACYT-Centro de Física Aplicada y Tecnología Avanzada, Universidad Nacional Autónoma de México, Boulevard Juriquilla 3001, Santiago de Querétaro, Qro, 76230, Mexico
[c] Instituto de Ingeniería y Tecnología, Universidad Autónoma de Ciudad Juárez, Av. del Charro No. 450 Nte. Col. Partido Romero, C.P. 32310, Mexico
[d] Centro de Investigación en Materiales Avanzados, SC, Miguel de Cervantes No. 120, Complejo Industrial Chihuahua, Chihuahua, 31136, Mexico

HIGHLIGHTS

- SilicaTitaniasilver fibers was obtained.
- Sol-gel and electrospinning processes is used.
- SERS on the detection of OTC was used.

GRAPHICAL ABSTRACT

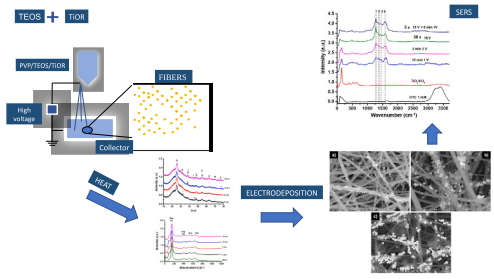

ARTICLE INFO

Keywords:
Oxytetracycline
Detection
SERS
Titania
Silica
Fibers
Silver nanoparticles

ABSTRACT

The presence of antibiotic residues such as oxytetracycline (OTC) in wastewater effluents has generated the need to monitor trace concentrations due to the development of bacterial resistance. Surface Enhanced Raman Spectroscopy (SERS) is a promising technique in detection and identification a low concentrations (ng/L) with no sample preparation. A fibrillar support Titania-Silica doped with silver particles was developed in the SERS technique focused on the detection of OTC. The ceramic fibers TiO_2SiO_2 obtained presented phases of Rutile, Anatase and Amorphous Silica with diameters of 335 ± 76 nm. The fibers were doped with Ag by electrodeposition, showed Ag nanoparticles with sizes from 30 nm to the formation of dendritic structures with sizes greater than 1 μm, depending on the time and voltage applied during synthesis. The support doped with Ag for 30 s at 19 V presented the highest amplification factor (AF) in SERS of 44 for the band at 1278 cm^{-1}.

1. Introduction

Antibiotics are pharmaceutical compounds used to treat and prevent infectious diseases in humans and animals. The agriculture industry uses antibiotics such as oxytetracycline to increase production, due to its effectiveness and low cost; therefore, in wastewater generated after treatment, antibiotic residues persist at trace concentrations; which contributes to the development of bacterial resistance [1];

* Corresponding author.
E-mail address: simon.reyes@uacj.mx (S.Y. Reyes-López).

https://doi.org/10.1016/j.matchemphys.2023.127968
Received 1 March 2023; Received in revised form 9 May 2023; Accepted 20 May 2023
Available online 30 May 2023

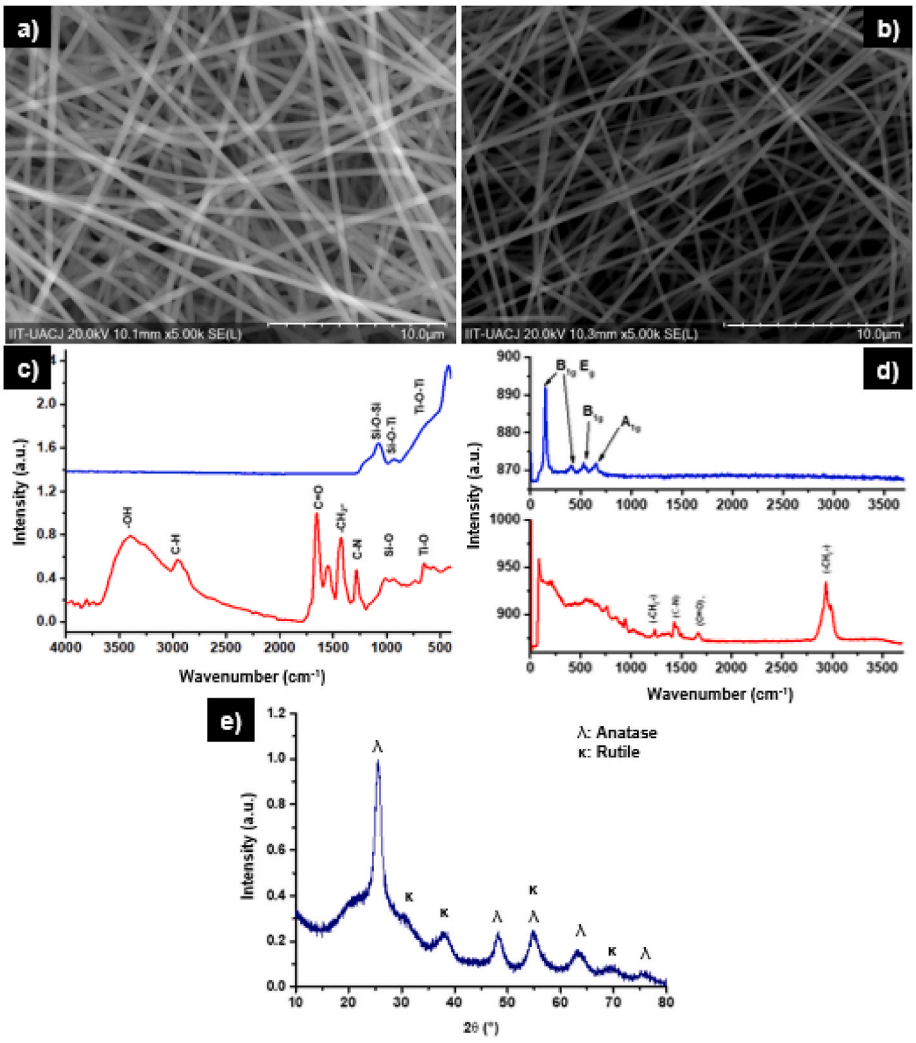

Fig. 1. SEM Images a)TiO_2SiO_2PVP fibers 5,000x, b)TiO_2SiO_2 fibers 5,000x, c) IR and d) Raman spectra of TiO_2SiO_2PVP y TiO_2SiO_2 fibers, e) XRD patterns of TiO_2SiO_2.

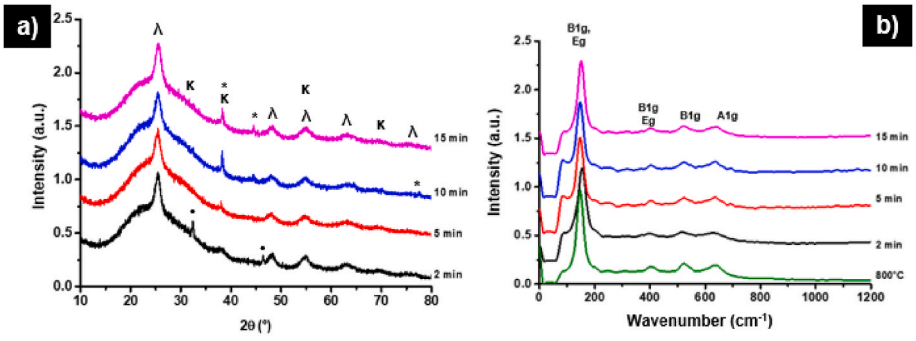

Fig. 2. a) XRD graph and b) Raman spectra of TiO_2SiO_2Ag supports.

Rivera-Jaimes et al., 2017). Monitoring of antibiotic residues in the environment is necessary. The High-Performance Liquid Chromatography Mass Spectrometry (HPLC-MS) is used for detection; however, require tedious sample treatments, are expensive, time-consuming, and have a low sensitivity to identify complex sample components. Here the relevance of developing simple, fast, and sensitive analytical methods, such as Surface Enhanced Raman Spectroscopy (SERS), a promising technique for the rapid detection of chemicals and biochemicals [2]; Reyes-López et al., 2017; [3,4]. The SERS technique is a sensitive detection method, provides information on the fingerprint of the analyte and is applied in various areas such as: chemistry, biology, environmental toxicology, monitoring of reactions etc. The technique consists in the generation of a more intense Raman spectrum by adsorbing the sample on a surface of metal particles (support); amplification factors (AF) of 10^6–10^{14} of the signals have been generated. The amplification effect is attributed to the formation of a surface resonance plasmon (PRS) on the metal particles and to the interaction between the surface of the support and the proximity of the analyte, through an

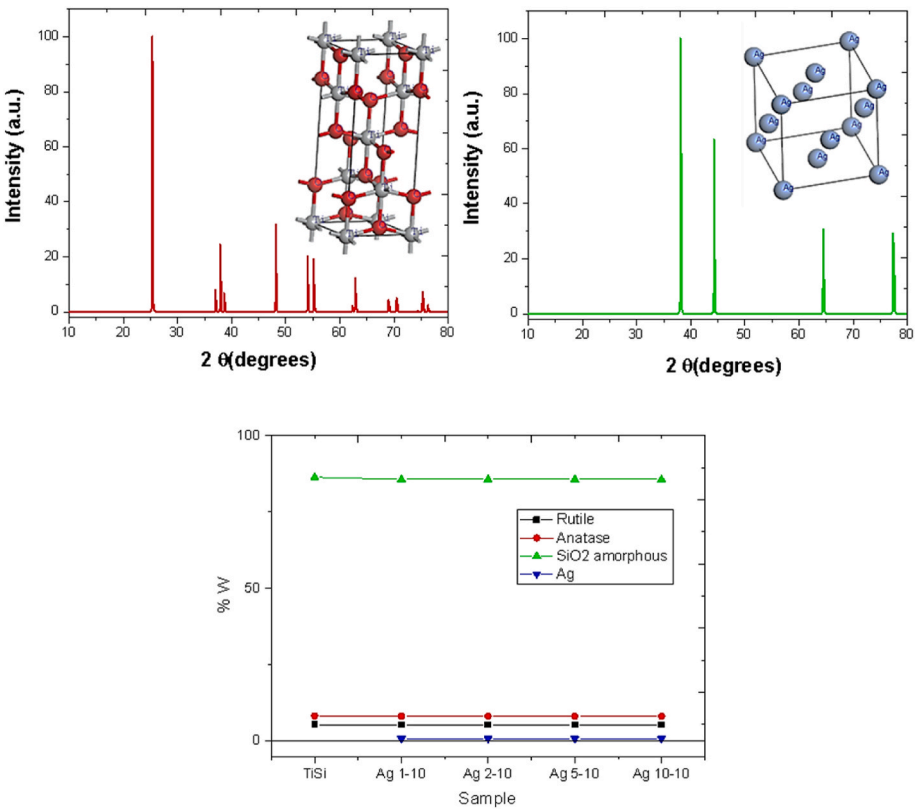

Fig. 3. Structures in the studied system and quantification phase analysis plot of the TiO_2SiO_2 and the TiO_2SiO_2Ag samples.

electromagnetic (EM) mechanism or a charge transfer mechanism (TC) [5,6].

Au, Ag and Cu are some of the most widely used noble metals for the development of SERS active supports, since they have a good increase in signals and have chemical stability. However, they are expensive and disposable [7]. It has been reported that the use of semiconductor materials with nanoparticles of noble metals as SERS supports has allowed to take advantage of the synergistic effect of the amplification mechanisms in addition to semiconductors such as TiO_2 gives the support the ability to be reusable due to its photocatalytic properties [4]. developed an Ag–TiO_2 support applied in the detection of quinolones in pM concentrations in addition to the support presented photocatalytic activity. Mixing TiO_2 with SiO_2 enhances the mechanical and photocatalytic properties of Titania, the high concentration of oxygen vacancies and surface defects can also act as charge recombination centers, which eventually decrease the photocatalytic activity, silica prevent recombination on TiO_2. Many works have been focused on the production of polymeric fibers with metallic nanoparticles as supports, but the disadvantage of having polymer in the matrix is the low mechanical resistance of the support, which makes it difficult to have a reusable SERS sensor [8]. The differences are very noticeable when comparing the organic polymer matrix, with the inorganic materials having good mechanical properties, chemical stability, and reusability. Menghui Wan et al., in 2021 report SiO2 fibers doped with noble metal nanoparticles, SiO2 fibers have unique properties, such as a large specific surface area, good thermochemical stability, biological safety, and non-toxicity and, in addition to its flexibility, do not present Raman bands, so it does not interfere with SERS detection [9]. The SiO_2 improve mechanical properties of the TiO_2 acting as a support and brings flexibility after calcination [4,10].

A SERS support of fibrillar structure acts as a base material where metal particles are deposited, avoiding agglomerations, and increasing the number of hot spots due to the high surface area [8]. SERS supports of polymeric fibers has been reported, polyacrylonitrile polymeric nanofibers with Ag SERS substrate for the detection of bacteria with detection limits of 10^{-9} M and polyurethane fibers covered with Au capable of monitoring biomarkers with pH measurement, useful supports for their flexibility, sensitivity, and high surface area [8,11]. However, the development of inorganic SERS substrates gives the material good thermochemical stability when irradiated with the laser. For example, a matrix of SiO_2 nanofibers coated with Ag nanoparticles presented a sensitivity of 10^{-11} M in the detection of pesticides and the quantitative detection of bacteria [10].

The techniques of sol-gel, electrospinning and electrodeposition have allowed the development of substrates of nanofibrous TiO_2–SiO_2 doped with dendritic nanoparticles of Ag, which have presented amplification factors of 27.03 in the detection of pyridine and violet crystal 1 nM [12,13]. Additional research on the mechanisms of spectroscopic amplification and the development of new supports are necessary in the detection of antibiotics. The use of SERS substrates of Au and Ag NPs with detection limits of 8.7×10^{-18} M to 9.9×10^{-4} M has been reported in the detection of OTC in aqueous solution; as well as the development of Au/PATP/SiO_2 and AgNPs/CNT-GO compounds with detection limits of 2.25×10^{-11} and 7.6×10^{-10} M [1,14–16]. In previous works we have optimized the mechanical resistance of titanium fibers by incorporating a glass matrix, avoiding the brittleness of the fibers when they are subjected to a sintering or densification process (Cabello-Ribota et al., 2021;; [17]. In this work, a SERS support Titania-Silica-Ag of nanofibrillar structure was developed, using the sol-gel, electrospinning, and electrodeposition techniques, to apply the material in the detection of oxytetracycline residues.

2. Materials and methods

Obtention of Sol-gel Titania-Silica (TiO_2–SiO_2); The ceramic fibers TiO_2SiO_2 were synthesized by means of the sol-gel technique. It was based on the precursors Tetraethylortosilicate (TEOS) and Titanium Tetraisopropoxide (TTIP), which were mixed with a 7:3 Ti/Si molar

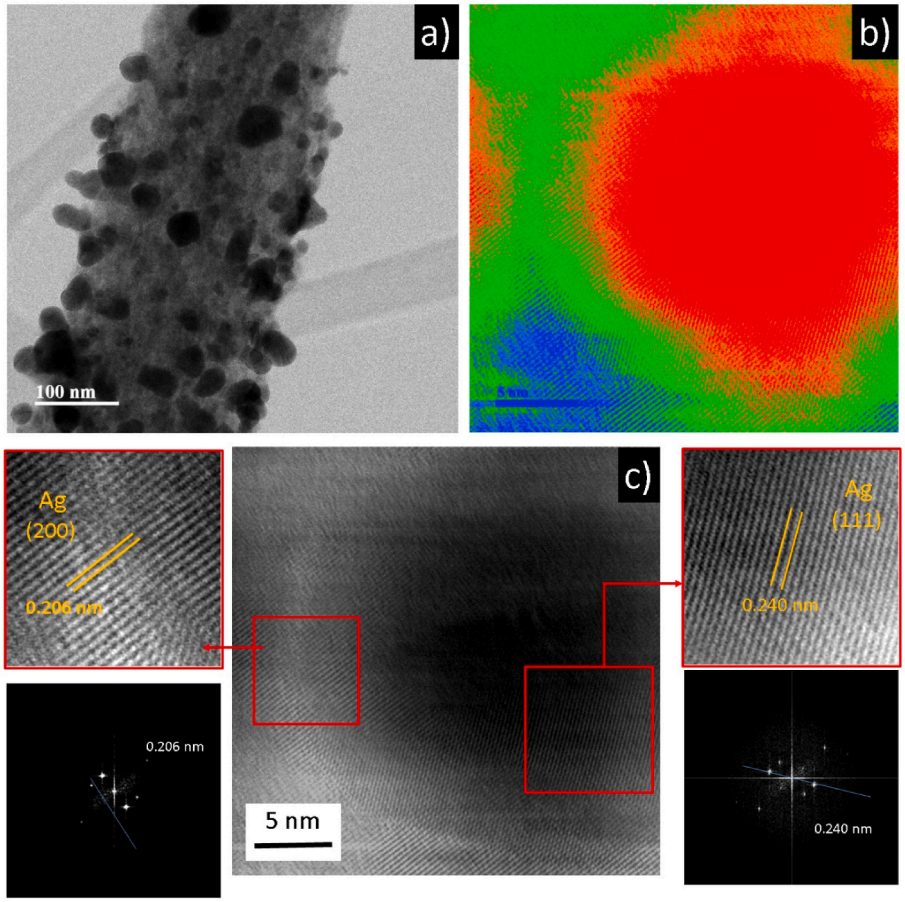

Fig. 4. a) TEM micrograph of SiO2–TiO2–Ag ceramic fibers, b) and c in the HRTEM mode.

ratio. Absolute ethanol was then added as a solvent and glacial acetic acid as a catalyst, in a 1:1:1 v/v ratio. The resulting sol-gel was stirred for 10 min, and 10% polyvinylpyrrolidone (PVP) was added in absolute ethanol with a ratio of 1:1 v/v, and stirred for 30 min, after the time elapsed, the TiO_2-SiO_2-PVP mixture was placed in a syringe to electrospinning [18].

Obtention of Fibers TiO_2-SiO_2-PVP Composite; The electrospinning parameters employed: voltage (8 kV), output distance from the syringe to the collector (10 cm), and a flow (0.5 mL/h) (Cabello-Ribota et al., 2021; [17]. The fibers obtained at ambient temperature (green fibers) were introduced to a desiccation stove at 100 °C for 24 h, to remove solvent and moisture. It was then given a heat treatment at 800 °C for 2 h on an electric muffle with a heating ramp of 5 °C/min.

Obtention of TiO_2–SiO_2–Ag support; The TiO_2–SiO_2 fibers were doped with silver nanoparticles by electrodeposition to obtain the SERS TiO_2–SiO_2–Ag supports. An electrolytic solution of $AgNO_3$ 10 mM was used, citric acid 1 M was aggregated as additive, a silver coin as anode and the fibers fixed to indium tin oxide (ITO) plastic with carbon tape as cathode. Doping times were varied from 5 s to 15 min, and the applied voltage of 1, 2 and 19 V [12].

Physical and chemical characterization of the composites; The fibers were characterized before and after being sintered. A JEOL JSM-6400 scanning electron microscope was used in order to know its morphology. To evaluate the composition, infrared spectroscopy and Raman were used. A Bruker Platinum ATR FTIR equipment was used, with a spectral range of 4000-400 cm^{-1} and 24 scans, and a Raman alpha300 WITec spectrometer with a 532 nm laser. TiO_2-SiO_2 fibers and Ag-doped supports were characterized with X-ray diffraction (XRD) to identify crystalline phases, an X'Pert PRO PANalytical equipment was used with Cu kα = 1.54, 20 kV, in a range of 2 θ from 10 to 80°.

Evaluation of signal amplification in Raman spectroscopy; The SERS evaluation was performed with a 1 mM oxytetracycline hydrochloride solution, 20 μL of the solution were taken and deposited on the TiO_2–SiO_2–Ag supports. From the OTC spectra obtained, characteristic bands of the analyte and the support were identified. The area under the curve of the bands of the OTC was compared with and without the support. The Raman alpha300 WITec spectrometer using a 532 nm laser was employed. The Amplification Factor (AF) was calculated with equation 1 [19]:

$$FA = (I_{SERS} / I_{SOL})(C_{SOL} / C_{SERS})$$

Where I_{SOL} and C_{SOL} correspond to the Raman intensity and concentration of the analyte without the presence of the support. While I_{SERS} and C_{SERS} corresponds to the SERS intensity and concentration of the solution on the support.

3. Results and discussion

3.1. Characterization of electrospunTiO_2SiO_2 fibers mats

The fibers obtained presented a cylindrical morphology, continuous, smooth, and free of defects, with diameters of 426 ± 78 nm in green (Fig. 1-a) and 335 ± 76 nm after being treated at 800 °C (Fig. 1-b) with a weight loss of approximately 67%. A heat treatment at a controlled rate of 5 °C/min does not generate changes in the morphology of the fibers after being treated at temperatures above 600 °C where they lose almost all organic matter according to the literature [13,18]. In the IR spectrum of TiO_2SiO_2PVP fibers (Fig. 1-c red) was identify absorption bands located at 3497 cm^{-1} attributed to the stretch vibration of the –OH group present in the solvent and moisture in the material before being

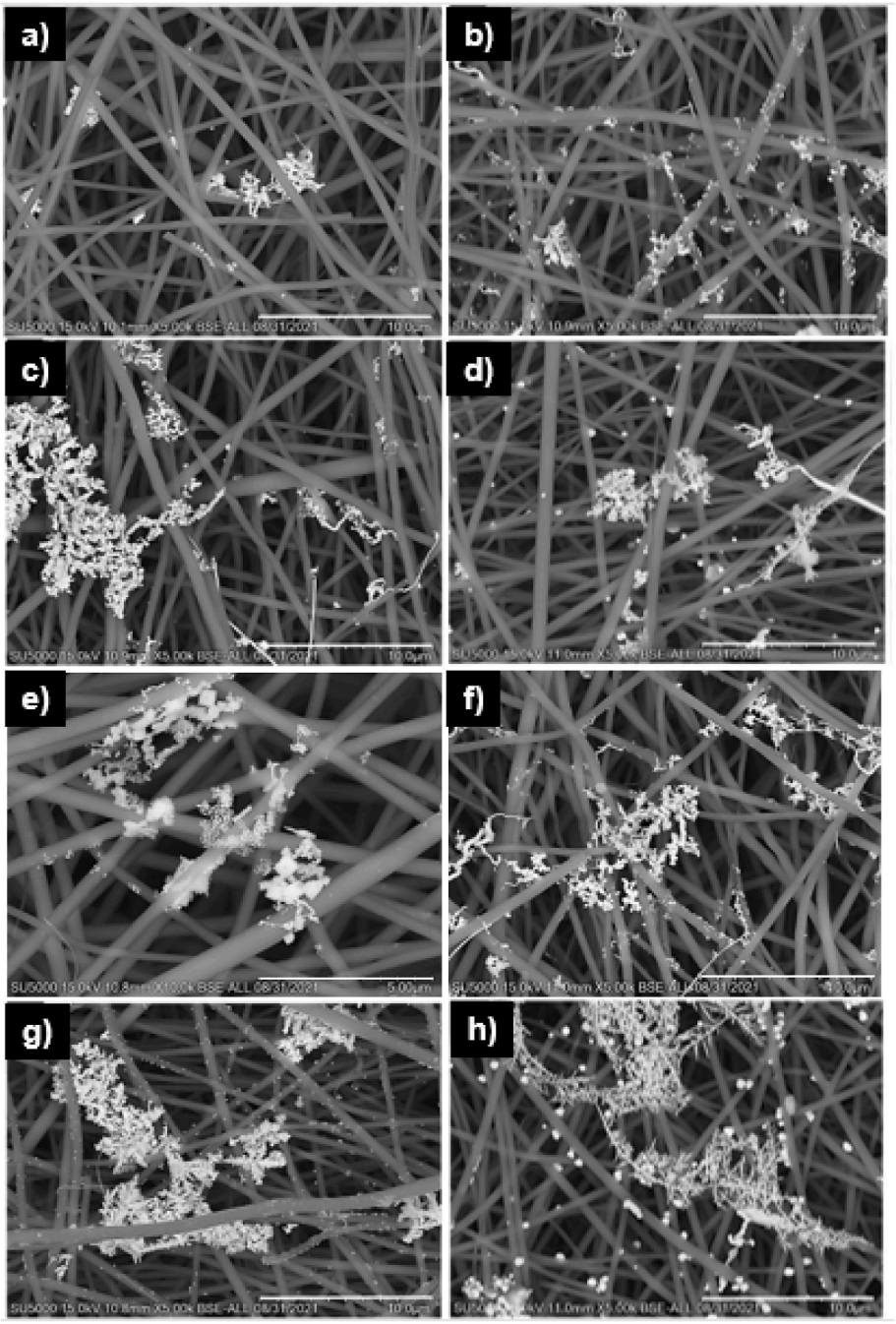

Fig. 5. SEM images TiO_2SiO_2Ag 5,000x doped with 1 V a) 2 min, b) 5 min, c) 10 min, d) 15 min and doped with 2 V e) 2 min, f) 5 min, g) 10 min and h) 15 min.

heat treated. In addition, characteristic bands of the PVP were identified, at 2953, 1421 and 1280 cm^{-1} correspond to asymmetric stretching vibrations and C–H deformation modes of CH_2, and to the C–N bending vibration present in the pyrrolidone of the polymer [20]. Low-intense and defined bands were identified at 940 and 420 cm^{-1} of bending vibrations of the Si–O and Ti–O bonds. In the spectrum of fibers sintered at 800 °C (Fig. 1 c blue) only bands located at 1204, 1082 and 936 cm^{-1} attributed to Si–O–Si bonds are identified, and the bands at 634 and 420 cm^{-1} that belong to Ti–O–Ti bonds [21,22]; Karagoz et al., 2019). The absence of the polymer bands is attributed to the thermal degradation of the PVP, which takes place from 250 °C. Fig. 1-d shows the Raman spectra of TiO_2-SiO_2-PVP (red) and TiO_2–SiO_2 (blue) fibers. The bands located at 2940 cm^{-1} a band attributed to the asymmetric stretch vibration of CH_2 in the PVP chain, at 1672 cm^{-1} to group C═O, 1494 cm^{-1} for the C–N bond, the bands located at 1428, 1367 and 1320 cm^{-1} are attributed to the bending vibration of CH_2 characteristics of PVP [23]. The vibration bands ascribed to the crystalline anatase phase at 409 and 526 cm^{-1} that correspond to B_{1g} and A_{1g} (Karagoz et al., 2019). The bands 409 and 611 cm^{-1} correspond to E_g and A_{1g} vibrational modes of the rutile respectively. The band located at 151 cm^{-1} corresponds to the vibrational motions E_g and B_{1g} belonging to both crystalline phases [24]. The formation of stable tetragonal anatase occurs below 700 °C, and a tetragonal phase of rutile, is formed close to 700 °C, the presence of both crystalline phases is due to an interference generated by silica during the formation of rutile, causing an increase in the temperature of formation of the anatase greater than 700 °C [25]. Fig. 1-e presents XRD analysis was possible to identify crystalline phases in ceramic fibers sintered at 800 °C. Peaks located at: 25.4°, 48.1°, 63.3°

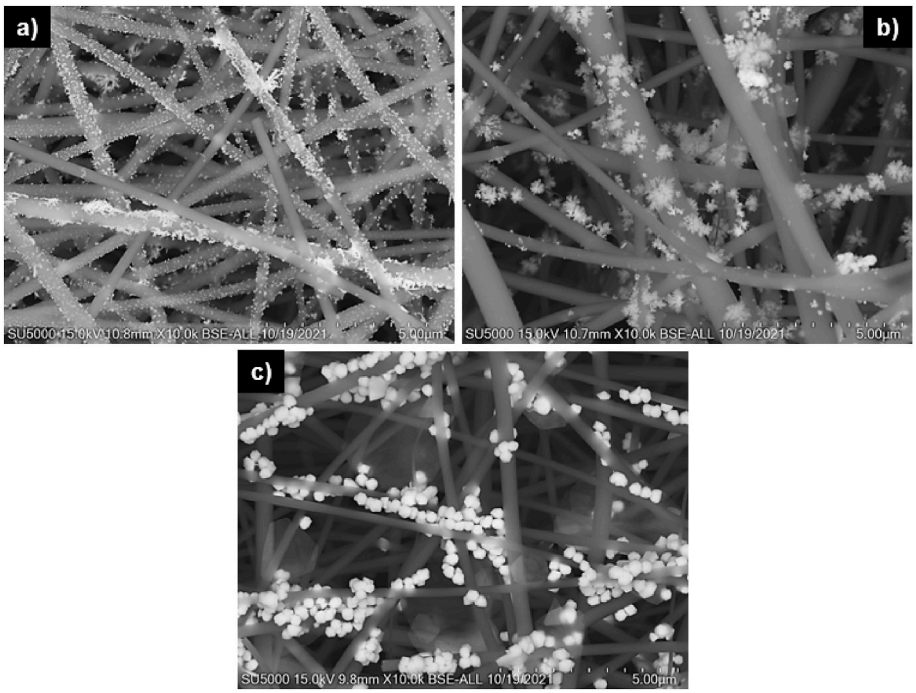

Fig. 6. SEM images TiO_2SiO_2Ag 10,000x doped with 19 V a) 5 s, b) 30 s, c) 5 s 19 V + 5 min 1 V

and 75.6° for the tetragonal anatase JCPDS [96-720-6076] are identified, associated with the planes (101), (200), (220) and (311); and peaks at 30.5°, 38.0°, 53.8° and 69.9° associated with the planes (110), (101), (211) and (301) of the tetragonal rutile JCPDS [96-900-4142], both crystalline phases characteristic of TiO_2. The present curvature of 20–30° is attributed to the presence of amorphous silica and the low intensity of the peaks indicates a low crystallinity in the fibers.

3.2. Characterization of TiO_2SiO_2Ag supports

Fig. 2-a shows the XRD graph of the fibers doped for 2, 5, 10 and 15 min with 2 V. Characteristic peaks of Ag were identified at 38.3°, 44.5°, 46.3° and 77.6° attributed to the planes (111), (200), (211) and (311) of the face centered cubic of silver JCPDS [01-087-0719], in the support doped for 2 min a peak is identified at 32.4° for the plane (111) characteristic of Ag_2O JCPDS [96-101-0487]. The Raman spectra of the TiO_2SiO_2Ag 2 V supports make it possible to identify bands of the crystalline phases anatase and rutile of Titania (Fig. 2-b). A decrease in the intensity of the band located at 145 cm^{-1} is observed, the remaining bands at 307, 409, 526 and 311 cm^{-1} are less defined with the increase in doping time. The widening of Raman signals is attributed to the interaction between Ag particles and ceramic fibers, as Ag is possibly introduced into the TiO_2 network [26,27].

3.3. Quantification phase analysis QPA

Fig. 3 shows the XRD patterns for the fibers and the structures in the studied system. The crystallographic analysis shows 8.176% for the anatase, 5.386% for rutile, 0.7845% silver FCC phase and 85.64% for amorphous silica. Confirming the low crystallinity of the fibers. The amorphous phase was obtained from the degree crystallinity calculations of the XRD patterns of the fibers. These results are consistent whit the initial composition of the fibers and with the notable amorphous phase observed in the range of 20–30° of the XRD patterns of the TiO_2SiO_2Ag fibers.

3.4. HRTEM analysis

Fig. 4 shows a TEM (4a) and HRTEM (4 b) images associated to the fibers doped with Ag, in this image is possible to observe the interphase of TiO_2 (anatase phase) and the Ag. The d spacing associated to the (111) planes of the Ag (0.241 nm) was fully identified (Fig. 4c). On the other hand, the interplanar distance of 0.184 nm was also measured and associated to the (020) planes of the anatase phase of the TiO2. The TEM and HRTEM image, confirms the Ag and TiO_2 presence phase. Is important to mentioning that the amorphous phase of SiO_2, is not possible to define by HRTEM images. However, the XRD patterns and the Raman spectroscopy analysis, support the TiO_2SiO_2Ag fibers formation.

The SEM images of the TiO_2SiO_2Ag supports shows Ag particles on the surface of the fibers with different morphologies and sizes, depending on the time and the applied voltage for electrodeposition. The supports 2 and 5 min 1 V presented small particles of 182.6 ± 64.9 nm in addition to clusters of particles of 0.8 ± 0.5 to 1.5 ± 0.5 μm (Fig. 5-a and b). Longer doping times of 10 and 15 min allowed the formation of wires (diameters of 281 ± 161 nm), and clusters of irregular particles of 13 μm approximately, and dendritic particles of 3.6 ± 2.9 μm (Fig. 5-c and d). The supports doped with 2 V shows particles of 61.8 ± 10.5 nm, strands, and cubes of 230 ± 108 nm, and dendritic particles (7–13 μm) were identified in the supports doped for 2 and 5 min (Fig. 5-e and f). With an increase the time to 10 and 15 min, many nucleated particles on the surface of the fibers were observed with sizes of 126.8 ± 27.7 nm, as well as clusters of irregular structures of 9–10 μm and well-defined dendrites from 3 to 20 μm (Fig. 5-g and h).

The voltage applied was increased to 19 V to search for a more uniform deposition. A deposition time of 5 s allowed to obtain nucleated particles of 26.7 ± 6.4 to 106.2 ± 42.9 nm distributed more uniformly on the fibers, as well as the formation of defined dendritic structures (Fig. 6-a). A time of 30 s allowed the formation of structures in the form of flowers made up of dendrites of 160.3 ± 36.8 nm (Fig. 6-b). To obtain more defined and more distributed particles, the 5 s 19 V support was given a second treatment of 5 min 1 V to promote the growth of the particles, however, the particles joined together, giving rise to spherical particles of 610.4 ± 104.2 nm (Fig. 6-c). The growth of Ag particles on

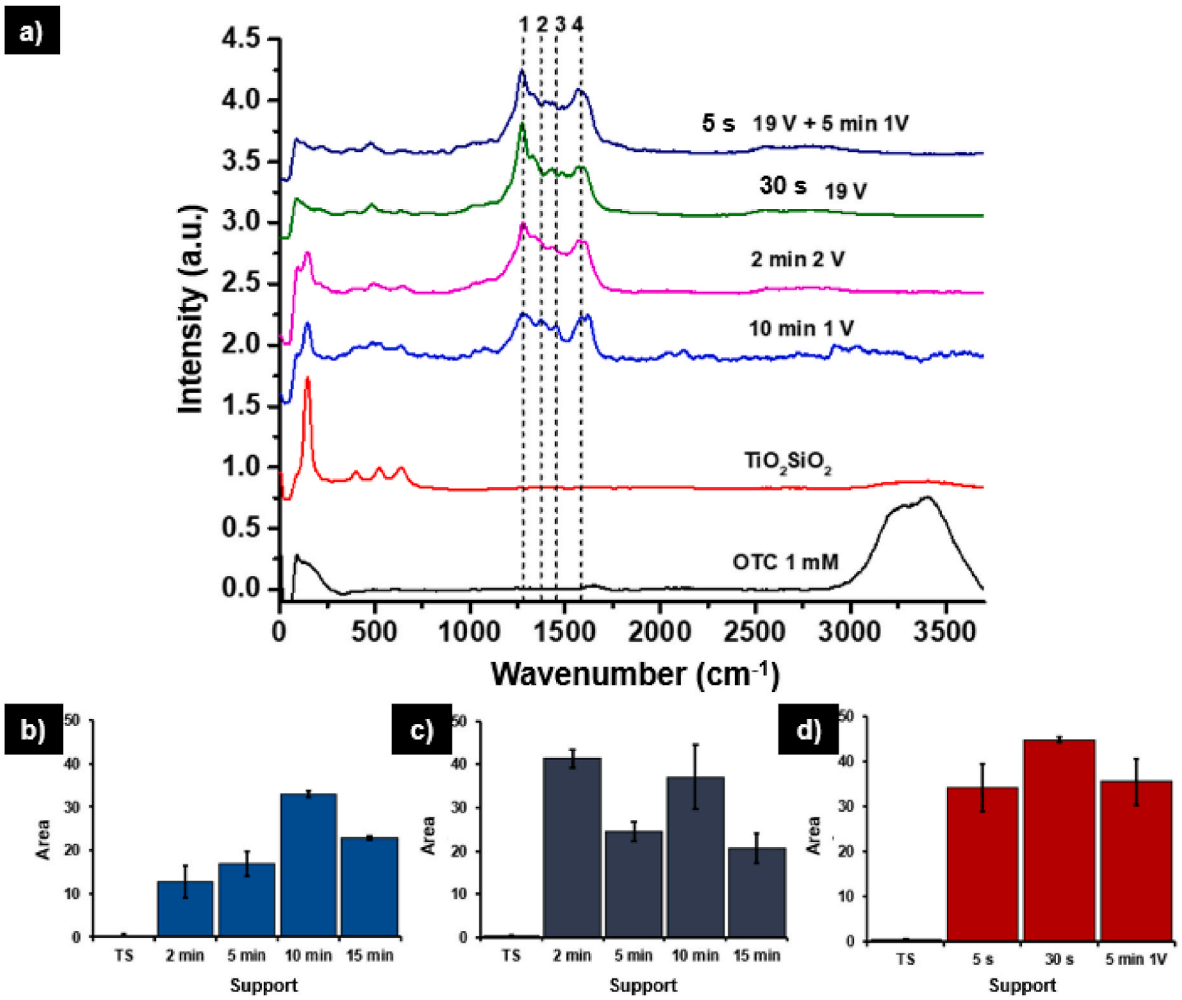

Fig. 7. a) Raman spectra of the OTC 1 mM and SERS spectras of the OTC on TiO_2SiO_2 fibers, TiO_2SiO_2Ag supports. Area under the curve of the band 1278 cm^{-1} for all supports doped with 1 V (b), 2 V (c) and 19 V (d).

Table 1
Amplification factors of the bands of the OTC by the supports doped with 1, 2 and 19 V

Band (cm^{-1})		TS	1 V				2 V				19 V		
			2 min	5 min	10 min	15 min	2 min	5 min	10 min	15 min	5 s	30 s	+5min 1 V
1	1278	0.40	12.6	16.7	32.2	22.4	40.6	24.1	36.4	20.24	33.7	44.1	34.9
2	1354	0.31	13.7	16.5	26.9	20.1	30.7	18.0	33.8	16.58	25.9	30.1	23.4
3	1471	0.32	11.8	16.7	25.2	13.8	31.5	16.2	21.3	15.85	24.8	25.9	24.6
4	1578	0.19	9.8	9.7	18.0	11.1	21.5	12.5	22.7	12.08	18.8	17.0	20.0

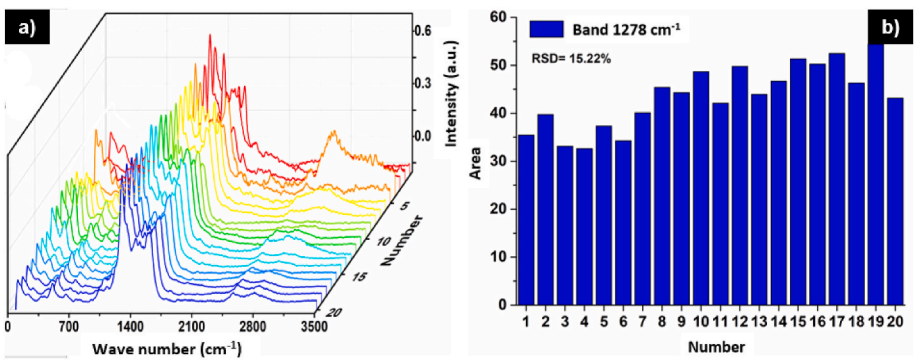

Fig. 8. a) SERS spectrum of OTC 1 mM on TiO2SiO2Ag 30s 19 V support from 20 different points, and b) The area distribution of the band at 1278 cm^{-1}..

the supports is explained by the diffusion limited aggregation (DLA) model, where it is mentioned that the electric field distributes the Ag^+ ions over the cathode, and the Ag^+ are reduced on the surface generating small particles called nucleus. The nucleus is mobilized until they reach specific sites where they are deposited, they are added successively and at the same time by the reduction of more Ag^+ on the particles they begin to grow since they are exposed to a higher concentration of Ag^+ than the fibers (Amin et al., 2020; [13].

The increase in the size and number of nucleated particles leads to the formation of structures with varied morphologies for the supports doped with 1, 2 and 19 V, at longer deposition times. The Ag has a face-centered cubic crystalline phase (fcc), a growth mechanism in the plane is favored (111), in such a way that in the initial stage of growth it gives rise to the formation of trunks or rods from which branches grow (Amin et al., 2020; Mandke et al., 2011), causing the formation of dendrites in high deposition times. The flat-directed growth (111) of the particles is also attributed to citric acid in the electrolytic solution. Citric acid is an additive, which adheres to specific faces in the crystal, directing growth and contributing to the development of morphologies such as strands and dendrites on supports (Amin et al., 2020, [28,29].

3.5. SERS evaluation of TiO_2SiO_2 and TiO_2SiO_2Ag supports

The SERS evaluation of the 1 mM OTC solution of the supports demonstrated the amplification capacity of the material (Fig. 7). In the Raman spectra of the OTC solution and of the TiO_2SiO_2 fibers, no characteristic bands of the antibiotic are identified, only a band at 3385 cm^{-1} that corresponds to an asymmetric stretch of the –OH present in the solution. In the SERS spectra of the OTC on the supports, the bands located at 1278 and 1354 cm^{-1} attributed to stretching vibrations of the C-OH and C–C bond respectively were identified; at 1483 and 1578 cm^{-1}, for the bending vibration of the C–H bond and C═C stretching vibrations present in the aromatic ring of the OTC [1]. Vibrational modes present in the phenolic group of the OTC molecule (Fig. 7-a). Fig. 7-b, c y d shows the area under the curve obtained for the band at 1278 cm^{-1} for all supports. The TiO_2SiO_2Ag supports present higher area values compare with TiO_2SiO_2 fibers. Table I shows the AF calculated for the 4 identified bands of the antibiotic on the TiO_2SiO_2 fibers and the supports 1, 2 and 19 V. Where the highest values were presented for the band at 1278 cm^{-1} of 32.25, 40.56, and 44.10 for the TiO_2SiO_2Ag 10 min 1 V, 2 min 2 V and 30 s 19 V supports. Compared with AF values of 2.9 and 15.7 for rhodamine 6G using Ag and Au nanoparticles respectively, values of 20 and 9.5 for crystal violet with a nanofibers of TiO_2SiO_2 and TiO_2SiO_2 dopped with copper, as well as ZnO nanorods and Coaxial Nanofibers SiO_2TiO_2Ag with AF values of 22 and 27 to 4-aminobenzenethiol (4-ABT) and pyridine; the values of AF obtained in this work are competitive (Cabello-Ribota et al., 2021; [17,30,31].

Fig. 8 shows the reproducibility study for the TiO_2SiO_2Ag 30s 19 V support from 20 Raman spectra taken at random points on a support (Fig. 6-a). The relative standard deviation (RSD) obtained for the area under the curve of the band at 1278 cm^{-1} was 15% (Fig. 6-b), close to 10, 12.8 and 14% RSD values reported for SERS supports of Ag particles which shows that the support has good uniformity according to literature [1,32,33].

The amplification of the Raman signal is attributed to the electromagnetic mechanism, which consists of the generation of a surface resonance plasmon (PRS) from the excitation of the free electrons of the metal particles. When the excitation wavelength resonates close to the absorption of the plasmon present in the nanoparticles a strong electromagnetic field was induced on the support and the Raman modes of the molecule near the surface are intensified. The generated PRS transfers its energy to the analyte due to its proximity to the substrate and the SERS effect is generated [3,7,17,34]. The presence of particles in form of dendrites generates many hot spots or spaces where PRS are located, these particles act as antennas favoring amplification [12]. The greatest amplification was presented in the doped support with 30 s 19 V, support where dendritic particles in the form of a flower were presented which are distributed more evenly, because more distributed particles contribute to the formation of more hot spots in the spaces between the particles. The amplified bands of the OTC correspond to the phenolic group of the antibiotic, indicating a closeness with the Ag particles, there is a possible electrostatic interaction between the aromatic ring and by bridges of H with the OH groups of the antibiotic molecule and the Titania-Silica-Ag composite [35–38].

4. Conclusions

Ceramic fibers TiO_2SiO_2 with diameters of 335 ± 76 nm was obtained, with the crystalline phases of Rutile and Anatase, according to the characterization of the fibers by SEM, IR, Raman and XRD. A higher voltage applied during electrodeposition allowed to obtain particles with more defined shapes and greater distributed along the fibrillar mats. The analysis of XRD for the supports show peaks of the Ag FCC structure formed by electrodeposition. The support doped for 30 s 19 V presented an FA value of 44 for the band at 1278 cm^{-1} an indicative of good SERS effect. The amplification is attributed to the formation of PRS on the hot spots of the dendritic particles, many nucleated particles on the surface and the chemical-physical interaction between the OTC and the support.

CRediT authorship contribution statement

Daniela Solorio-Grajeda: Conceptualization, Methodology, Formal analysis, Investigation, Resources, Data curation, Writing – original draft, Writing – review & editing. **Álvaro de Jesús Ruíz-Baltazar:** Methodology. **Manuela Alejandra Zalapa-Garibay:** Methodology. **Erasto Armando Zaragoza-Contreras:** Methodology. **Simón Yobanny Reyes-López:** Conceptualization, Methodology, Formal analysis, Investigation, Resources, Data curation, Writing – original draft, Writing – review & editing, Visualization, Supervision, Project administration, Funding acquisition, All authors have read and agreed to the published version of the manuscript.

Declaration of competing interest

The authors declare that they have no known competing financial interests or personal relationships that could have appeared to influence the work reported in this paper.

Data availability

Data will be made available on request.

References

[1] L.L. Qu, Y.Y. Liu, M.K. Liu, G.H. Yang, D.W. Li, H.T. Li, Highly reproducible Ag NPs/CNT-intercalated GO membranes for enrichment and SERS detection of antibiotics, ACS Appl. Mater. Interfaces 8 (41) (2016) 28180–28186.
[2] L. He, M. Lin, H. Li, N. Kim, Surface-enhanced Raman spectroscopy coupled with dendritic silver nanosubstrate for detection of restricted antibiotics, J. Raman Spectrosc. 41 (2009) 739–744.
[3] F. Soto-Nieto, R. Farías, S.Y. Reyes-López, Sol–gel and electrospinning synthesis of sili-ca–hydroxyapatite–silver nanofibers for SEIRAS and SERS, Coatings 10 (10) (2020) 910.
[4] W. Wang, Q. Sang, M. Yang, J. Du, L. Yang, X. Jiang, B. Zhao, Detection of Several Quinolone Antibiotic Residues in Water Based on Ag-TiO2 SERS Strategy, Science of the Total Environment, 2019.
[5] M.F. Cardinal, E.V. Ende, R.A. Hackler, M.O. McAnally, P.C. Stair, G.C. Schatz, P. P. Van Duyne, Expanding applications of SERS through versatile nanomaterials engineering, Chem. Soc. Rev. (2017) 3886–3903.
[6] D.A. Skoog, F.J. Holler, S.R. Crouch, in: D.F. Cengage Learning (Ed.), Principles of Intrumental Analis, sixth ed., 2008.
[7] W. Zheng, W. Tian, X. Liu, Q. Zhang, C. Zong, J.P. Lai, W. Zhao, In situ photochemical deposition of Ag nanoparticles on polyester fiber membranes as flexible SERS substrates for sensitive detection of sodium saccharin in soft drinks, Microchem. J. 164 (2021), 106003.

[8] Y. Yang, Z. Zhang, M. Wan, Z. Wang, Y. Zhao, L. Sun, Highly sensitive surface-enhanced Raman Spectroscopy Substrates of Ag@ PAN electrospinning nanofibrous membranes for direct detection of bacteria, ACS Omega 5 (31) (2020) 19834–19843.
[9] Menghui Wan, Haodong Zhao, Zhihua Wang, Xueyan Zou, Yanbao Zhao, Lei Sun, Fabrication of Ag modified SiO2 electrospun nanofibrous membranes as ultrasensitive and high stable SERS substrates for multiple analytes detection, Colloid and Interf. Sci. Commun. 42 (2021), 100428, https://doi.org/10.1016/j.colcom.2021.100428.
[10] M. Wan, H. Zhao, Z. Wang, X. Zou, Y. Zhao, L. Sun, Fabrication of Ag modified SiO2 electrospun nanofibrous membranes as ultrasensitive and high stable SERS substrates for multiple analytes detection, Colloid and Interf. Sci. Commun. 42 (2021), 100428.
[11] M. Chung, W.H. Skinner, C. Robert, C.J. Campbell, R.M. Rossi, V. Koutsos, N. Radacsi, Fabrication of a wearable flexible sweat pH sensor based on SERS-active Au/TPU electrospun nanofibers, ACS Appl. Mater. Interfaces 13 (43) (2021) 51504–51518.
[12] B.S. Cabello-Ribota, R. Farías, S.Y. Reyes-López, Surface enhanced infrared absorption studies of SiO2–TiO2–Ag nanofibers: effect of silver electrodeposition time on the amplification of signals, Crystals 11 (5) (2021) 563.
[13] J. Roque-Ruiz, S.Y. Reyes-López, H. Martínez-Máynez, A. Zalapa-Garibay, A. Arizmendi-Moraquecho, R. Farias, Surface enhanced Raman spectroscopy in nanofibers mats of SiO2-TiO2-Ag, Results Phys. (2017) 2520–2527.
[14] H. Li, Q. Chen, M.M. Hassan, X. Chen, Q. Ouyang, Z. Guo, J. Zhao, A magnetite/PMAA nanospheres-targeting SERS aptasensor for tetracycline sensing using mercapto molecules embedded core/shell nanoparticles for signal amplification, Biosens. Bioelectron. 92 (2017) 192–199.
[15] F. Meng, X. Ma, N. Duan, S. Wu, Y. Xia, Z. Wang, B. Xu, Ultrasensitive SERS aptasensor for the detection of oxytetracycline based on a gold-enhanced nano-assembly, Talanta 165 (2017) 412–418.
[16] A.G. Fá, F. Pignanelli, I. López-Corral, R. Faccio, A. Juan, M.S. Di Nezio, Detection of oxytetracycline in honey using SERS on silver nanoparticles, Trac. Trends Anal. Chem. 121 (2019), 115673.
[17] D. Solorio-Grajeda, J. Torres-Pérez, N. Medellín-Castillo, S.Y. Reyes-López, Surface enhanced Raman spectroscopy effect and acicular growth of copper structures on Titania-Silica fibers, Inorg. Chem. Commun. 150 (2023), 110484, https://doi.org/10.1016/j.inoche.2023.110484.
[18] X. Wang, J. Zhu, L. Yin, S. Liu, X. Zhang, Y. Ao, H. Che, Fabrication of Electrospun Silica–Titania Nanofibers with Different Silica Content and Evaluation of the Morphology and Osteoinductive Properties, vol. 100, Wiley Periodicals Inc., 2012, pp. 3511–3517.
[19] C. Tan, Z. Zhang, Y. Qu, L. He, Ag2O/TiO2 nanocomposite heterostructure as a dual functional semiconducting substrate for SERS/SEIRAS application, Langmuir 33 (22) (2017) 5345–5352.
[20] I.A. Safo, M. Werheid, C. Dosche, M. Oezaslan, The role of polyvinylpyrrolidone (PVP) as a capping and structure-directing agent in the formation of Pt nanocubes, Nanoscale Adv. 1 (8) (2019) 3095–3106.
[21] P. Larkin, IR and Raman Spectroscopy Principles and Spectral Interpretation, Elsevier, San Diego, 2011.
[22] G. Socrates, Characteristic Group Frequencies Tables and Charts, John Wiley & Sons, LTD, New York, 2004.
[23] H. Mao, J. Feng, X. Ma, C. Wu, X. Zhao, One-dimensional silver nanowires synthesized by self-seeding polyol process, J. Nanoparticle Res. 14 (6) (2012) 1–15.
[24] M. Henderson, A. Gibaud, J.-F. Bardeau, J. White, An X-ray reflectivity study of evaporation-induced self-assembled titania-based films, J. Mater. Chem. (16) (2006) 2478–2487.
[25] S.W. Lee, Y.U. Kim, S.S. Choi, T.Y. Park, Y.L. Joo, S.G. Lee, Preparation of SiO2/TiO2 composite fibers by sol–gel reaction and electrospinning, Mater. Lett. 61 (3) (2007) 889–893.
[26] C. Han, V. Likodimos, J.A. Khan, M.N. Nadagouda, J. Andersen, P. Falaras, D. D. Dionysiou, UV–visible light-activated Ag-decorated, monodisperse TiO 2 aggregates for treatment of the pharmaceutical oxytetracycline, Environ. Sci. Pollut. Control Ser. 21 (20) (2014) 11781–11793.
[27] A. Pandikumar, R. Ramaraj, TiO2-Au nanocomposite materials modified photoanode with dual sensitizer for solid-state dye-sensitized solar cell, J. Renew. Sustain. Energy 5 (4) (2013), 043101.
[28] K.S. Choi, Shape control of inorganic materials via electrodeposition, Dalton Trans. (40) (2008) 5432–5438.
[29] J. Chu, Y. Zhao, S.H. Li, W.W. Li, X.Y. Chen, Y.X. Huang, Y. Xiong, A highly-ordered and uniform sunflower-like dendritic silver nanocomplex array as reproducible SERS substrate, RSC Adv. 5 (5) (2015) 3860–3867.
[30] K. Kim, K.L. Kim, K.S. Shin, Raman spectral characteristics of 4-aminobenzenethiol adsorbed on ZnO nanorod arrays, Phys. Chem. Chem. Phys. 15 (2013) 9288–9294.
[31] P. Wen, F. Yang, C. Ge, S. Li, Y. Xu, L. Chen, Self-assembled nano-Ag/Au@ Au film composite SERS substrates show high uniformity and high enhancement factor for creatinine detection, Nanotechnology 32 (39) (2021), 395502.
[32] M.U. Amin, L. Zhang, R. Hao, D. Zhang, H. You, J. Fang, Electrochemical growth of dendritic silver nanostructures as facile SERS substrates, CrystEngComm 23 (3) (2021) 694–699.
[33] E. Wiercigroch, A. Kisielewska, A. Blat, A. Wislocka, I. Piwoński, K. Malek, Photocatalytical decoration of thin titania coatings with silver nanostructures provides a robust and reproducible SERS signal, J. Raman Spectrosc. 50 (2019) 1649–1660, https://doi.org/10.1002/jrs.5707.
[34] M. Moskovits, Surface-enhanced spectroscopy, Rev. Mod. Phys. 57 (3) (1985) 783.
[35] M. Brigante, P.C. Schulz, Remotion of the antibiotic tetracycline by titania and titania–silica composed materials, J. Hazard Mater. 192 (3) (2011) 1597–1608.
[36] A.L. Filgueiras, D. Paschoal, H.F. Dos Santos, A.C. Sant'Ana, Adsorption study of antibiotics on silver nanoparticle surfaces by surface-enhanced Raman scattering spectroscopy, Spectrochim. Acta Mol. Biomol. Spectrosc. 136 (2015) 979–985.
[37] S. Karagoz, N.B. Kiremitler, M. Sakir, S. Salem, M.S. Onses, E. Sahmetlioglu, E. Yilmaz, Synthesis of Ag and TiO2 modified polycaprolactone electrospun nanofibers (PCL/TiO2-Ag NFs) as a multifunctional material for SERS, photocatalysis and antibacterial applications, Ecotoxicol. Environ. Saf. 188 (2020), 109856.
[38] J.A. Rivera-Jaimes, C. Postigo, R.M. Melgoza-Alemán, J. Aceña, D. Barceló, M.L. de Alda, Study of pharmaceuticals in surface and wastewater from Cuernavaca, Morelos, Mexico: occurrence and environmental risk assessment, Sci. Total Environ. 613 (2018) 1263–1274.